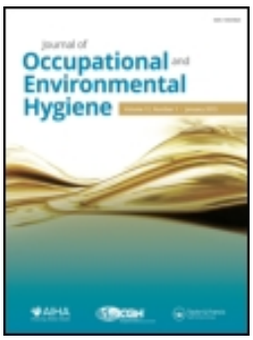

Journal of Occupational and Environmental Hygiene

ISSN: 1545-9624 (Print) 1545-9632 (Online) Journal homepage: http://www.tandfonline.com/loi/uoeh20

# Development of the chemical exposure monitor with indoor positioning (CEMWIP) for workplace VOC surveys

K.K. Brown, P.B. Shaw, K.R. Mead, R.J. Kovein, R.T. Voorhees & A.R. Brandes

**To cite this article:** K.K. Brown, P.B. Shaw, K.R. Mead, R.J. Kovein, R.T. Voorhees & A.R. Brandes (2016) Development of the chemical exposure monitor with indoor positioning (CEMWIP) for workplace VOC surveys, Journal of Occupational and Environmental Hygiene, 13:6, 401-412, DOI: 10.1080/15459624.2015.1125488

**To link to this article:** http://dx.doi.org/10.1080/15459624.2015.1125488

Accepted author version posted online: 19 Jan 2016.
Published online: 06 Apr 2016.

JOURNAL OF OCCUPATIONAL AND ENVIRONMENTAL HYGIENE
2016, VOL. 13, NO. 6, 401–412
http://dx.doi.org/10.1080/15459624.2015.1125488

Taylor & Francis
Taylor & Francis Group

# Development of the chemical exposure monitor with indoor positioning (CEMWIP) for workplace VOC surveys

K.K. Brown[a], P.B. Shaw[a], K.R. Mead[a], R.J. Kovein[a], R.T. Voorhees[b], and A.R. Brandes[c]

[a]Division of Applied Research and Technology, National Institute for Occupational Safety and Health (NIOSH), Cincinnati, Ohio; [b]University of Cincinnati, Cincinnati, Ohio; [c]MeasureNet Technology, Ltd., Cincinnati, Ohio

**ABSTRACT**

The purpose of this article was to research and develop a direct-reading exposure assessment method that combined a real-time location system with a wireless direct-reading personal chemical sensor. The personal chemical sensor was a photoionization device for detecting volatile organic compounds. The combined system was calibrated and tested against the same four standard gas concentrations and calibrated at one standard location and tested at four locations that included the standard locations. Data were wirelessly collected from the chemical sensor every 1.4 sec, for volatile organic compounds concentration, location, temperature, humidity, and time. Regression analysis of the photo-ionization device voltage response against calibration gases showed the chemical sensor had a limit of detection of 0.2 ppm. The real-time location system was accurate to 13 cm ± 6 cm (standard deviation) in an open area and to 57 cm ± 31 cm in a closed room where the radio frequency has to penetrate drywall-finished walls. The streaming data were collected and graphically displayed as a three-dimensional hazard map for assessment of peak exposure with location. A real-time personal exposure assessment device with indoor positioning was practical and provided new knowledge on direct reading exposure assessment methods.

**KEYWORDS**

3-D hazard map; direct-reading method (DRM); exposure assessment; photo-ionization detector (PID); real-time location system (RTLS); volatile organic compounds (VOCs)



## Introduction

The exposure of workers to volatile organic compounds (VOCs) is a serious health problem.[1] The problem is compounded by the fact that traditional surveys to detect hazardous compounds can take weeks to organize, carry out, and report results. An alternative approach, advocated in recent years, has been to establish direct-reading methods (DRMs) for use in the workplace that provide instantaneous measurement of exposure concentration and location to both the exposed person and anyone remotely monitoring the device with supervisory responsibility. The goal of this study iswas to develop a portable DRM apparatus using a photoionization detector (PID) combined with a real-time location system (RTLS) in a device small enough to attach to a worker. In this way, the worker's exposure can be monitored in real time and associated with a specific location.

A proprietary ultra-wide-band (UWB) radio-frequency (RF) RTLS (Ubisense, Denver, CO) was chosen on the premise that it would provide the best positioning accuracy and could be connected with a chemical sensor. UWB methods use software algorithms to track UWB RF beacons and calculate locations. Hui et al. conducted a survey of wireless indoor positioning systems and concluded that proprietary UWB systems provided the best accuracy.[2]

Adding indoor RTLS technology to a direct reading instrument as a means of assessing exposure is a new concept that may advance the exposure sciences. Lee et al. used geostationary positioning system (GPS) technology in a DRM for outdoor occupational exposure assessment,[3] and Nieto et al. used a GPS RTLS to improve safety in open pit mining.[4] Unfortunately, GPS technology does not work indoors, where most U.S. manufacturing is done, and GPS accuracy is not good enough for indoor measurements (7.8 m at a 95% confidence, according to GPS.gov). Indoor positioning systems (IPSs) have been gaining use for tracking medical patients. Boulos and Berry used various IPS technologies in the healthcare industries, concluding that successful RTLS deployment lies in picking the right RTLS options and solutions for the applications or problems at hand.[5] Huang et al.

**CONTACT** K.K. Brown krb1@cdc.gov Division of Applied Research and Technology, National Institute for Occupational Safety and Health, 4676 Columbia Parkway MS-R7 Cincinnati, OH 45226

Color versions of one or more of the figures in the article can be found online at www.tandfonline.com/uoeh.

used radio frequency identification (RFID) devices sewn in workers' vests to detect their location as they walked through specific work areas with chemical monitors during the workday. The researchers called this a Radio Frequency Identification Exposure Monitoring System (RFEMS).[6] However, this was not a real-time method, and it had low location accuracy, providing a broad VOC measurement from a stationary sensor in the center of a work area. Another radio frequency technique, ultra-wide-band positioning, is gaining market share because of its higher accuracy (15–30 cm).[7] Hoping to produce a more accurate exposure measurement system, we chose a proprietary Ubisense UWB RTLS coupled with a custom-built chemical sensor.

Sensors vary according to what is being measured: chemical, sound, radiation, heat, humidity, VOC, etc. Personal size VOC sensors include electrochemical,[8] photoionization,[9] and tuning fork sensors.[10] This project used a classic photoionization detector (PID), miniaturized for VOC detection. The PID has been used for decades for detecting VOCs in the work environment and it is commercially available.[9] Its simple technology has allowed it to be miniaturized. The transition of the PID from a GC detector in the 1970s to handheld detector today was not well documented in the literature. Commercially available handheld miniature PIDs cannot be used for compliance monitoring because they are not accurate and precise enough, but they can be useful as survey tools.[11] Thus, this chemical exposure monitor with indoor positioning (CEMWIP) method was not designed for compliance monitoring but for surveying exposure, by coupling an RTLS to a personal PID. One advantage of a nonspecific detector is its ability to monitor most occupational releases of VOCs.

In Canada, the annual average concentration of volatile organic compounds (VOCs) in outdoor air for 2012 was 53.9 parts per billion carbon (ppbC) as reported by Environment Canada.[12] The U.S. Environmental Protection Agency's (EPA) Office of Research and Development's Total Exposure Assessment Methodology (TEAM) Study (Volumes I–IV, completed in 1985) reported indoor VOC levels for about a dozen common organic pollutants to be 2–5 times higher inside homes than outside. Thus, relative to the outdoor 53.9 ppbC reference, indoor air ranged 108–270 ppbC. The PID in this evaluation had an analytical range of 200–10,600 ppb for isobutylene, so this method should be able to monitor at and above average concentrations of indoor VOCs. To evaluate the CEMWIP system, the PID VOC sensor was calibrated against four standard gases and later tested against the same standards while implementing an experiment design. The indoor positioning component was calibrated against one standard location and later tested against four while implementing the same experiment design.

This method may fall under the NIOSH US patent 7191097, Method, apparatus, and system for assessing conditions,[3,13] in that this invention is directed to a method, apparatus, and system for assessing conditions at one or more locations over time. The difference between the method and apparatus described in this paper and those described in the original patent is that ours successfully tackled the difficult problems of a practical indoor positioning system for these types of systems whereas the patent documented outdoor GPS.

## Methods

### *Materials*

The RTLS was purchased from Ubisense as a research and development package that contained location software, 4 UWB sensors, 5 RF tags, 5 tag circuit chips, and sensor mounting hardware (Ubisense Inc., Denver, CO). The UWB sensors were RF detectors, herein after referred to as antennas. An additional antenna was purchased later.

The five antennas measured the time difference of arrival (TDOA) and angle of arrival (AOA) of an RF signal emanating from the personal device. The five antennas were placed around the periphery of the work area wall near the ceiling, pointing toward the center of the room. Data cables connected the sensors in series, starting from a master timing unit to the last slave unit. The extra-peripheral equipment needed for the RTLS included a laptop, server, GS108P power-over-ethernet (PoE) switches (Netgear, San Jose, CA), and Cat5e Ethernet cables. The Ubisense positioning software was installed on a Dell Precision M6600 17.3″ laptop workstation featuring a 2.2 GHz quad-core processor with professional-grade graphics (Dell Corporate Headquarters, Plano, TX). Shielded Cat5e cables were used to couple in between antennas, and unshielded Cat5 cables were used to connect from individual antennas to the PoE switch. The laptop was connected via the PoE switch to complete the RTLS.

The CEMWIP system consisted of the commercially available Ubisense RTLS and a custom-made wireless personal PID and software (MeasureNet Technology, Cincinnati, OH). The two systems combine indoor positioning with a personal VOC detector for workplace exposure assessment. The system had a remote real-time laptop display of location and exposure for second-person monitoring and a personal real-time display for first-person monitoring. Both personal sensor position and VOC concentration were remotely monitored on the laptop in real time.

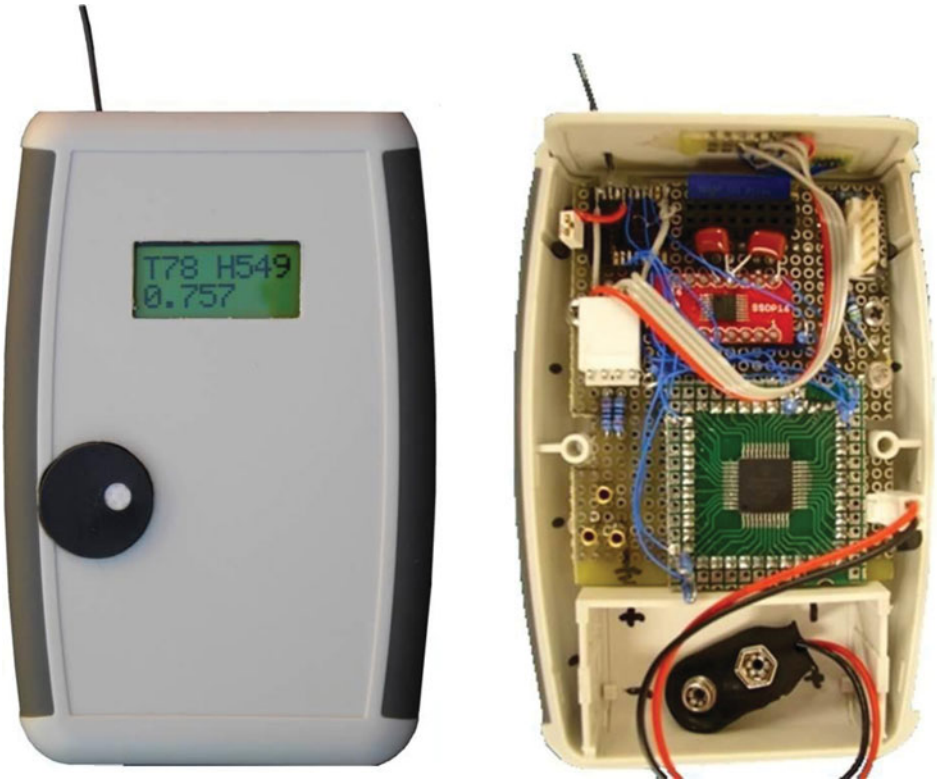


**Figure 1.** Alpha version of the CEMWIP wireless sensor, front and inside.

### *Personal sensor*

Figure 1 shows the alpha version of the CEMWIP personal wireless chemical sensor, designed and assembled by MeasureNet Technology. Although there are small "pocket" PIDs sensors are commercially available, none of them have interface ports that allows for connection via Wi-Fi, and so this unit was custom built. This version of the personal PID had a liquid crystal display (LCD); two rows, eight characters per row (Newhaven Display Intl, Inc., Elgin, IL). The battery used was a 9-volt, rechargeable 520-mAh Li-Polymer. This CEMWIP device contains a miniature PID the size of a small coin protruding out the front and a temperature and humidity sensor embedded in the top of the case. The PID voltage was digitized with a 24-bit ADC part AD7799 (Analog Devices, Norwood, MA). An 8-bit microprocessor (PIC18F46K2) was programmed to control the data flow (Microchip, Chandler, AZ). The data output was sent to LCD display and RF transceiver chip, RFD21813 (RF Digital Corporation, Irvine, CA). The unit measured 3 × 5 × 1 in, weighed about 4 oz, and could be clipped onto a belt. The wireless transceiver data antenna was at the top of the unit.

The personal monitor contained two sensors: PID for VOCs, and CMOS chip for temperature, and humidity. However, only the VOC monitor was evaluated for accuracy and precision in house. The PID used to detect VOCs was a Baseline-Mocon #043-235 with a 10.6-eV (116.9-nm) krypton lamp and a detection range of 0.2–20 ppm. The lamp's magnesium chloride window provided ultraviolet transmission from 0.12–7.0 µm. The miniaturized PID was about the size of a U.S. 5-cent coin, with a diameter of 20.4 mm and weight of <8 g. This sensor can be battery operated, with a 64–300 mW power consumption. Baseline-Mocon provides five 10.6-eV detectors, with range limits of 10,000, 2,000, 200, 20, and 0.2 ppm; this evaluation used the detector with a range of 0.2–20 ppm. However, the detectors are interchangeable, and thus, different ranges can be used (Baseline Inc., Lyons, CO).

Temperature and humidity were monitored with a silicon band-gap temperature sensor integrated into a Sensirion SHT11 complementary metal oxide semiconductor (CMOS) chip, which also monitored humidity by means of capacitive change on polymers. The SHT11 chip used in the CEMWIP personal unit was advertised as the world's smallest with ±3% accuracy for relative humidity and ±0.4°C precision for temperature.[15] This chip consumes only 80 µW of energy while delivering 12 bits of analog to digital converter (ADC) data over a two-wire interface and only has four leads (Sensirion, Zurich, Switzerland).

### Peripheral materials

The sensor data were sent in real time from the CEMWIP unit to a RFD21743 remote base station (RF Digital Corporation, Hermosa Beach, CA). This transceiver system had a range of 2,000 ft by line of sight and meets Federal Communication Commission (FCC) regulations. The sensor digital data were sent by USB cable from the RFD21743 to a mini-computer. The mini-computer contained a Linux server that in turn parsed the data to the remote laptop for processing and displaying.

A Mini-Box M300-LCD mini-computer housed the CEMWIP software and the RFD21743 transceiver base (Mini-Box.com, Fremont, CA). The mini-computer ran an Ubuntu Linux operating system. Custom software on the mini-computer collected the digital sensor data through the RFD21743 interface, calculated the VOC concentration, plotted the concentration on the floor plan, and added color to the location dot in proportion to VOC concentration. The mini-computer was in turn connected to the laptop that calculated position with Ubisense software. Mini-computer software provided network communication with the laptop Ubisense software collecting location data and merging it with chemical sensor data and redisplaying both on the laptop. The mini-computer stored all data in a MySQL database (www.mysql.com) and facilitated database access with a web site programmed in *PHP: Hypertext Preprocessor* language under Apache Web Server software (httpd.apache.org).

Two Netgear eight-port network switches with four power-over-ethernet (PoE) ports were used to couple the five RTLS antennas and the minicomputer to the laptop that housed the Ubisense locations system software.

An Ubisense series 7000 RF tag was used to track the location of the CEMWIP personal sensors. This UWB RF beacon was externally attached to the CEMWIP device and contained its own battery and had unique digital ID. The tag weighed 6 g and emitted a 5.8–7.2 GHz UWB RF pulse to be received by the wall-mounted sensors; the pulse was at such a low energy level that it was exempted from licensing under FCC Part 15 regulations. The RF tag also contains a RF communication chip at 2.4-GHz for 2-way communication with the UWB wall-mounted antenna for remote laptop control of tag, i.e., on and off, pulse rate, sleep mode, battery life, and ID. The internal chip was embedded inside the wireless sensor circuitry of beta CEMWIP versions.

### Experimental design

As shown in Figure 2, the CEMWIP system was assembled in the NIOSH Ventilation Laboratory in Cincinnati, Ohio, a 480-$m^2$ space that simulated a small industrial worksite, including isolated breakout workrooms. Four RF antennas (blue letters A–D) were mounted around the upper peripheral wall of the room so all antennas would "see" the RF signal from test location #1. A moving tag has to be seen by at least two wall sensors for a location to be calculated. Each wall antenna was connected to the computer by single Cat5 data cables (magenta lines in Figure 2) laid over the ceiling. The sensors received RF pulses, determined the AOA, and transmitted the AOA data to the computer. The wall antennas also had to be connected, in a series of daisy-chained shielded Cat5e cables, from the master timing antenna to the remote computer, as shown in green in Figure 2. These cables carried (TDOA) information.

The antennas were located at *x, y, z* locations of (1) 6.23, 0.212, 2.692; (2) 0.206, 10.598, 2.483; (3) 2.02, 22.316, 3.024; (4) 20.037, 13.696, 2.369; and (5) 19.935, 0.5128, 2.323 m. The upper left corner of the floor plans in Figure 2 was designated as the 0, 0, 0 Cartesian coordinate The antenna arrays were aligned to have azimuths centered toward location #1 and elevations of 35°. The antennas had a horizon tilt of zero.

The remote monitoring components of the system, consisting of two network switches, a laptop computer, and an RF base station with mini-computer, were located in WKSTAT-3 area (brown rectangle in Figure 2). These components were used to acquire data, calculate sensor position and gas concentration, and display data in real time. The data switches consisted of two NETGEAR GS108P-100NAS four-port PoE switches coupled to connect five data lines from the five independent sensors. The PoE routers powered the antennas. The minicomputer ran custom CEMWIP software that coupled the chemical data with RTLS data for display on the floor plan.

Four test locations, shown as numbered red dots in Figure 2 and listed on Table 1, were marked on the floor and measured precisely with a Leica DISTO D2 Laser Distance Measurer; the upper left corner of the room was used as the point of origin (0, 0). The laser device was capable of measuring precision to a millimeter, and one location was used for calibration and four points for evaluating the RTLS. The RTLS was calibrated against location #1 and tested against all four location. The four locations were measured as being the following distances (in meters) from the origin: (1) 12.872, −8.226, 0.888; (2) 4.315, −10.369, 0.888; (3) 2.646, −18.385, 0.888; and (4) 16.836, −10.995, 0.888. Locations 2, 3, and 4 were in rooms and thus were also used to test the penetration ability of the RF radiation through the walls to the antennas. The *z* locations used during the experiment did not vary and were designated as the height of the cart (0.888 m).

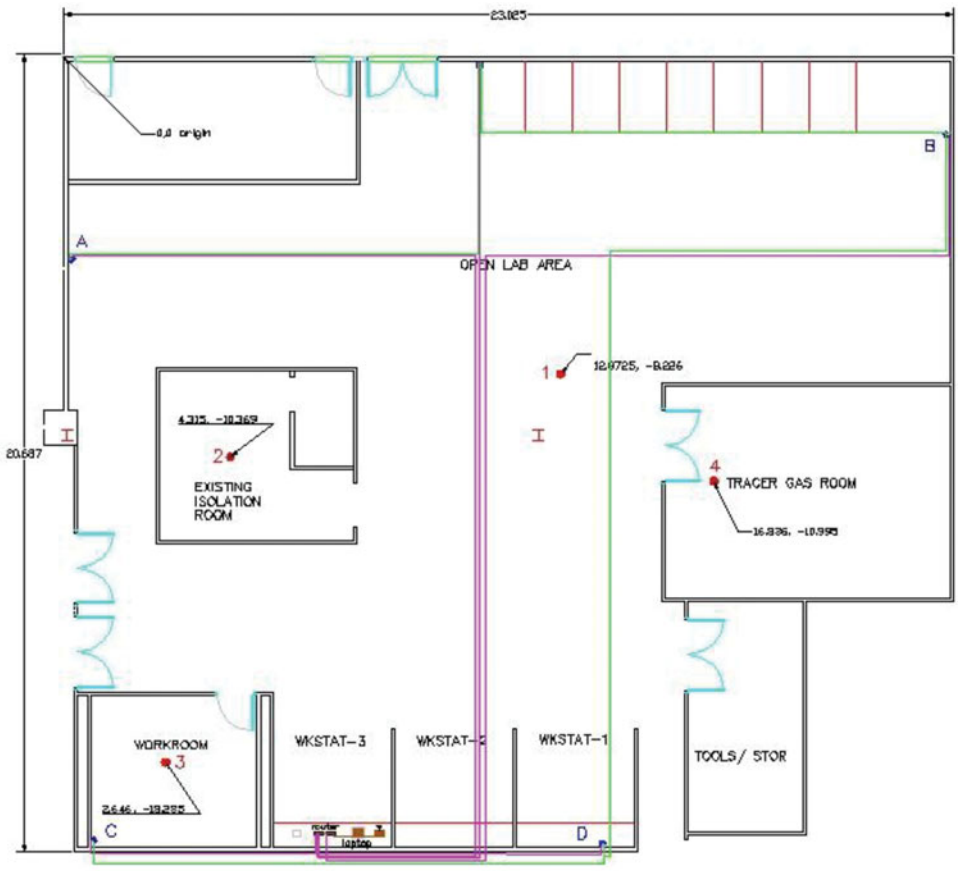


**Figure 2.** Floor plans showing the NIOSH ventilation laboratory, RTLS system cabling, and test locations.

Data from the random combinations of location and concentration were analyzed by regressions analysis to estimate accuracy and precision. Figure 3 shows an Ubisense tag banded to the CEMWIP sensor on a mobile cart. Also visible are two calibration cylinders and tripods, indicating calibration location #1 in front and #4 in the back room. Not visible are the other two calibration locations that were used in this evaluation. The room was set up for one run at a time with four location and calibration gas combinations. During each run, the cart was pushed from location to location according to a predetermined, randomized schedule. At each location, a gas delivery wand from the gas cylinder was placed over the PID and the calibration gas was released for 2 min to ensure reading equilibrium. After 2 min of dosing, the cart was pushed to the next location, reaching four locations per run. Between each run, the cylinders were rearranged to the next run combinations.

**Table 1.** Experimental design permutations of location and concentration.

| Run | Trial | Isobutylene Concentration (ppm) | Test Location |
|---|---|---|---|
| 1 | A | 0 | 3 |
| 1 | B | 0.994 | 4 |
| 1 | C | 0.101 | 1 |
| 1 | D | 10.6 | 2 |
| 2 | A | 0 | 1 |
| 2 | B | 10.6 | 4 |
| 2 | C | 0.994 | 2 |
| 2 | D | 0.101 | 3 |
| 3 | A | 0 | 4 |
| 3 | B | 0.101 | 3 |
| 3 | C | 10.6 | 2 |
| 3 | D | 0.994 | 1 |
| 4 | A | 0 | 4 |
| 4 | B | 0.994 | 1 |
| 4 | C | 10.6 | 3 |
| 4 | D | 0.101 | 2 |

Four compressed-gas cylinders were used to calibrate the PID. Three tanks of isobutylene in nitrogen certified at 0.101 ± 10%, 0.994, and 10.6 ppm ± 5% were purchased as both calibration and test gases (Matheson Tri-Gas Inc., Twinsburg, OH). The fourth cylinder contained ultra-high-purity nitrogen only. A PVC tube wand was constructed to deliver gases to the PID. The wand was made from 9 in of ¾ inch PVC tubing with an end-cap nipple that accepted Tygon tubing from the gas cylinder. The open end of the wand fit over the PID to deliver a stream of known-concentration isobutylene. A ring of eight 1/16-in pressure-relief holes were drilled near the open end of the wand to prevent sensor overpressure from the calibration gas cylinder.


**Figure 3.** The NIOSH ventilation laboratory, staged with two standard gas cylinders at locations 1 and 4, with a tagged sensor on a mobile cart ready for experiment.

The four standard gas concentrations were released twice at each of the four locations, and only at the test locations. When the personal sensor reached the test location a gas-regulated cylinder was opened that had a gas delivery wand made from Tygon tubing and ¾-in PVC tube. The wand was placed over the PID for 2 min, and then the gas was turned off. The CEMWIP sensor monitored VOCs continuously before, during, and after gas delivery. The order of concentrations at the test locations was randomized. The evaluation took place within a 3.5-hr period. The normal response of a PID to a VOC change is exponential with an asymptotic approach to a plateau with the highest response being the end measurement. It was the end of plateau response that was used for experimental measurements.

## *Data analysis method*

The accuracy of the PID was assessed in two ways. First, the measured concentration of the isobutylene was regressed against the actual concentration. The goal was to determine how close the intercept was to 0.0 and the slope to 1.0. Second, the accuracy, precision, and bias of the PID were determined according to the approach described by Kennedy et al.[14] and Bartley.[15] As noted by Bartley, the relationship between bias (B), accuracy (A), and precision ($T_{RSD}$) may be formulated as

$$\alpha = \Phi\left[\frac{B+A}{T_{RSD}}\right] - \Phi\left[\frac{B-A}{T_{RSD}}\right], \tag{1}$$

where $\Phi$ is the standard normal distribution function and $T_{RSD}$ (a measure of precision) is the true relative standard deviation. Thus, the accuracy defines a range over which a fraction $\alpha$, say 0.95, of responses occurs. The accuracy, $A$, may be estimated with a formula presented in Bartley's report:[15]

$$A = \left\{ \begin{array}{ll} \dfrac{\mu}{2}(1+\alpha) \cdot \left[B^2 + T_{RSD}^2\right]^{1/2}, & |B| < \dfrac{T_{RSD}}{u_\alpha} \\ |B| + u_\alpha \cdot T_{RSD}, & otherwise \end{array} \right\}. \tag{2}$$

The actual details of the calculations, taken from Kennedy et al.,[14] are given in the Appendix. Another way of expressing accuracy, $A$, in this context is that it defines a range, centered at the target concentration, which contains a given fraction (usually 0.95) of the responses and this range is $((1\text{-}A)T_c, (1+A)T_c)$ where $T_c$ is the target concentration.

Accuracy of the Ubisense RTLS was assessed by performing a regression analysis of the coordinate values obtained from the RTLS on coordinate values obtained from the laser distance-measuring device against the test locations values. With the data, regressions were performed for the $x$ and $y$ coordinates separately. If the RTLS accurately measured distances, then such a regression

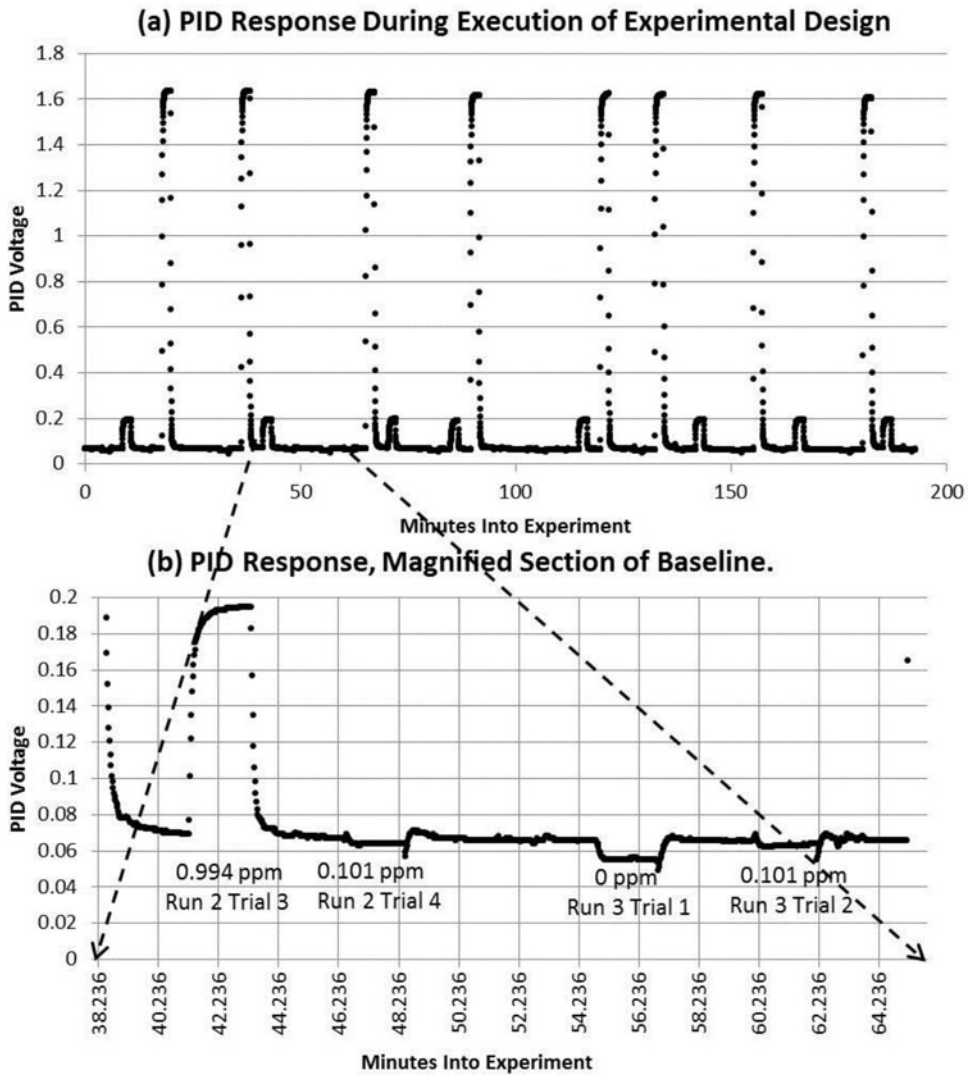


**Figure 4.** PID response vs. time.

should show an intercept, $\beta_0$ of 0.0 and a slope, $\beta_1$, of 1.0. In other words, the actual (laser) and estimated (RTLS) distances should be the same.

The limit of detection (LOD) for the PID in the experiment was determined by a regression of voltage on the actual concentration. The slope of the regression line, $b_1$, and the root mean square of the errors, $s$, were needed to determine the LOD, which was estimated as $\frac{3_s}{b_1}$.

## Results

A total of 8,064 lines of data were collected with eight unique fields: Tag No., Temperature, Humidity, PID (V), Tag Time, *X*, *Y*, and *Z*. At each position calibration point shown in Figure 2, the sensor was exposed to calibration gases for 2 min. During these 2 min, the peak PID response was used for analyzing the accuracy and precision of the system, and the data from in-between test locations were not used. For the 4-D plot, all 8,064 lines were used.

Figure 4a is the *X*-*Y* scatterplot of PID response in millivolts vs. time, collected continuously, one data point each 1.4 sec, during the entire evaluation period. The 8 tallest peaks are the responses to 10.6-ppm isobutylene, and the 8 peaks at about 0.2 volts are responses to 0.994 ppm. The responses to the 0.101 and 0 ppm are buried in the baseline. Figure 4b is a magnified section showing responses for a 0.101- and 0.0-ppm standard and background. The response to 0.101 and 0.0 ppm standards were identified by correlating their time stamp and location data, not shown, to the experimental design to identify their concentration. The PID response was used to identify test time periods for the location data. For example, with use of Excel software, the cursor can be put over the peak seen for 0.994 ppm in the magnified plot and the time can be read: 43.28 min, 0.195 V. The 2-min time period of 43.28–41.28 min before this peak was used to average location data found in that range for regression analysis. The zero calibration gas produced a response

**Table 2.** Regression analysis of measured concentrations vs. actual concentrations.

| Parameter | Estimate | Standard Error | 95% Confidence Interval |
|---|---|---|---|
| $\beta_0$ (intercept) | − 0.0255 | .0125 | − 0.0511 to 0.000047 |
| $\beta_1$ (slope) | 1.0726 | .0025 | 1.0675 to 1.0777 |

below background. The electrical spikes seen at the end of some 2-min periods were caused by the gas delivery wand touching the sensor as it was removed.

The chemical sensor was calibrated by estimating the linear relationship between sensor millivolts and isobutylene concentration. A linear regression analysis yielded the relationship $y = 6.81x - 0.342$ ($R^2 = 0.9999$), where $y$ is the isobutylene concentration in ppm and $x$ is the observed sensor reading in millivolts.

## PID: Precision, bias, and accuracy

A regression of the measured concentrations of the chemical on the actual concentrations applied yielded the results shown in Table 2 ($R^2 = 0.9998$).

The estimate of the intercept does contain 0.0; thus, we do not reject the hypothesis that $\beta_0 = 0.0$. The estimated slope is quite close to 1.0 (although technically we would reject the hypothesis that $\beta_1 = 1.0$), suggesting that the PID is providing measurements close to the actual concentrations. Figure 5 shows a graph of the regression line and the data.

The precision, bias, and accuracy, as calculated by the method of Bartley[14] and Kennedy et al.,[13] were as follows. The precision and bias were determined not to be homogeneous for the three concentrations. Therefore, precision was taken to be the maximum precision for the three concentrations and bias was taken to be the maximum bias for the three concentrations, following the

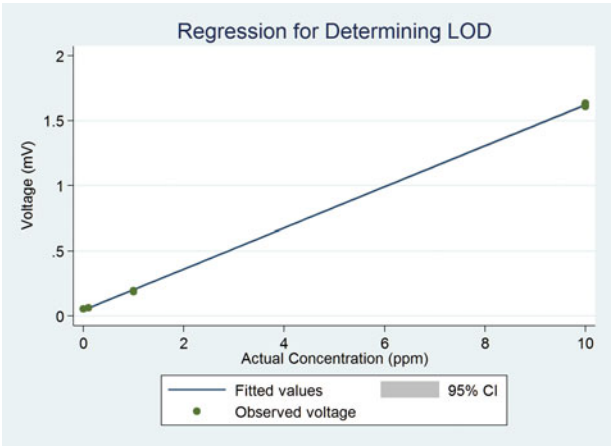


**Figure 5.** Linear regression of the measured voltage against actual concentrations.

**Table 3.** Regression of the RTLS measurements vs. laser measurements.

| X Parameters | Estimate | Standard Error | 95% Confidence Interval |
|---|---|---|---|
| $\beta$0 (intercept) | 1.1772 | 0.1167 | 0.9389 to 1.4156 |
| $\beta$1 (slope) | 0.9384 | 0.0075 | 0.9231 to 0.9536 |
| **Y Parameters** | **Estimate** | **Standard Error** | **95% Confidence Interval** |
| $\beta_0$ (intercept) | 0.5359 | 0.1874 | 0.1531 to 0.9187 |
| $\beta_1$ (slope) | 1.0333 | 0.0149 | 1.0028 to 1.0638 |

recommendations in NIOSH.[16] The precision was estimated to be 7.22%. The bias was estimated to be 13.57%.

Finally, the point estimate of accuracy was calculated using the second option in (2), noting that $|B| > \frac{T_{RSD}}{u_{\varepsilon\varepsilon}}$, with $|\beta| = 0.1357$ and $\frac{T_{RSD}}{u_\alpha} = \frac{.0722}{1.6449}$. Thus, accuracy was estimated, with use of $\alpha = 0.95$ and $|B| + u_\alpha \cdot T_{RSD}$, to be 0.2544, 25.44%. The LOD was actually above the concentration that was nominally 0.1 ppm, thus we would expect poor accuracy for that concentration. If we exclude the data for that concentration then the accuracy was much smaller (5.22% [smaller is better]) and the bias was much smaller (−2.27%).

It is interesting to note that one can plug the estimated values of $A$, $B$, and $T_{\mathrm{RSD}}$ into Bartley's Equation (1) as a sort of validation of the results presented here and Bartley's method. Recall that theoretically $\Phi[\frac{B+A}{T_{RSD}}] - \Phi\ [\frac{B-A}{T_{RSD}}] = 0.95$ One finds, using the experimentally determined values of B, A, and $T_{\mathrm{RSD}}$, that

$$\Phi\left[\frac{B+A}{T_{RSD}}\right] - \Phi\left[\frac{B-A}{T_{RSD}}\right] = 0.95, \qquad (3)$$

thus providing not only a validation of the estimates presented here for bias, accuracy, and precision but also a rather remarkable validation of Bartley's method for calculating $A$, as given in (2).

In Figure 5, the measurements obtained for each level of known concentration (0, 0.1, 1.0, and 10.0) were very close together. Although there appears to be only four or five separate data points on the graph, there are actually four sets of data points with eight points in each set. The eight points in each set are tightly grouped. The 95% confidence interval for the fitted values is shown, but it is so narrow that it is somewhat difficult to discern.

The regression of voltage on concentration yielded $s =$ .00861 and $b_1 = .1575839$ with $R^2 = 0.9998$. The limit of detection is $\frac{3s}{b_1} = \frac{3(.00860893)}{.15758395} = 0.164$ or 0.2 ppm.

## RTLS accuracy

A regression of the RTLS measurements on the laser measurements for the $x$ and y coordinates yielded the estimates of their intercepts and slopes, as shown in Table 3 with $R^2$ of 0.9981 and 0.9938, respectively.

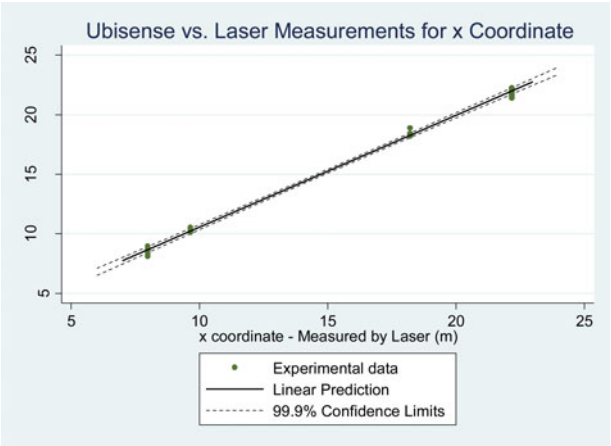


**Figure 6.** Graph of the regression line for the X coordinate.

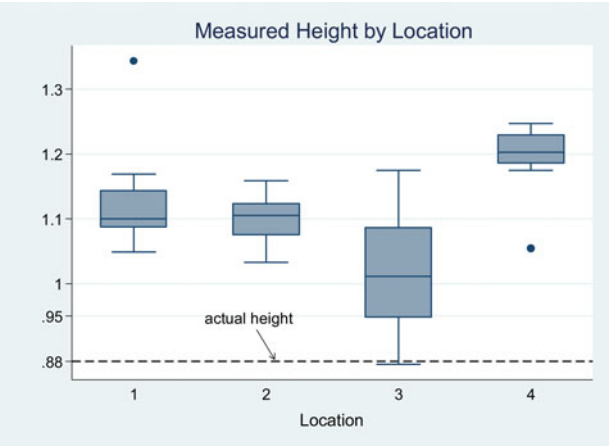


**Figure 8.** Box plots of Z-axis measurements.

For the X coordinate, the $Y$ intercept had a 95% confidence interval between 0.9389 and 1.4156 not containing 0.0; thus we reject the hypothesis that $\beta_0 = 0.0$. Similarly, for the slope, the 95% confidence interval, 0.9231–0.9536, does not contain 1.0; thus, we reject the hypothesis that $\beta_1 = 1.0$. However, the estimated values of the intercept and slope are close to 0.0 and 1.0, respectively, suggesting that the RTLS is providing measurements close to the actual distances. Figure 6 shows a graph of the regression line and the data. The LOD for measuring $X$ coordinate distance is $\frac{3s}{b_1} = (3 * 0.2483)/.9384 = 0.794$ m, where $s$ is the root mean square error, meaning the method should discern down to 79 cm for the $x$ coordinate.

Similarly in the case of the Y coordinate, the estimated value of the intercept has a confidence interval (0.1531–0.9187) that does not contain 0.0; thus, we reject the hypothesis that $\beta_0 = 0.0$. Likewise, the estimated value of the slope has a confidence interval (1.0028–1.0638) that does not include 1.0; thus, we reject the hypothesis that $\beta_1 = 1.0$. Note, however, that the estimated values of the intercept and slope are close to 0.0 and 1.0, respectively,

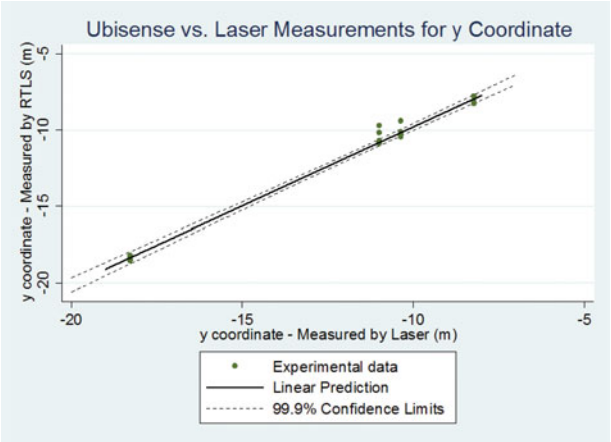


**Figure 7.** Graph of the regression line for the y coordinate.

suggesting that the RTLS is providing measurements close to the actual distances. Figure 7 shows the regression line and data points for the y coordinates. The LOD for measuring the $Y$ distance is $\frac{3s}{b_1} = (3 \times 0.31995)/1.0333 = 0.929$ m, where $s$ is the root mean square error, meaning the method should discern down to 93 cm for the $y$ coordinate.

The actual $z$ value (height) never changed, because the RTLS was attached to the cart. Thus, there was no reason to do a regression. Box plots of the data from the four locations are shown in Figure 8. The box plots suggest rather strongly that the measurements of the RTLS were systematically exceeding the true value of 0.88. A sign test rejected the hypothesis that the measured values were equal to 0.88 ($p = 0.0000$), thus providing evidence of inaccuracy in the RTLS's measurement of the $z$ coordinate.

Figure 9 shows another way of visualizing the accuracy and precision of the RTLS, by plotting the $x$, $y$ coordinates provided by the personal sensor during the 2-min stays at the four test locations during run 1. Each location provided 630 samples. The $z$-axis was not plotted because it was experimentally kept constant, but the $z$-axis measurement data can be found in Figure 8. Test location 1 showed the best accuracy and precision, with only a few dots being seen, because so many were plotted on top of each other. The average was plotted in the center of the true location (diamond). Location 1 data in Table 4 show that its measurement has the smallest absolute error of 13 cm and standard deviation of 6 cm. Location 1 had direct line of sight to the antennas while locations 2, 3, and 4, had to penetrate walls for the RF to reach the antennas. Location 2 is an example of the worst accuracy and location 4 the worst precision. The RTLS was calibrated to location 1 before the evaluation started. Thus, the real-time location system was accurate to 13 cm ± 6 cm (standard deviation) in an open area (locations 1) and on an average of

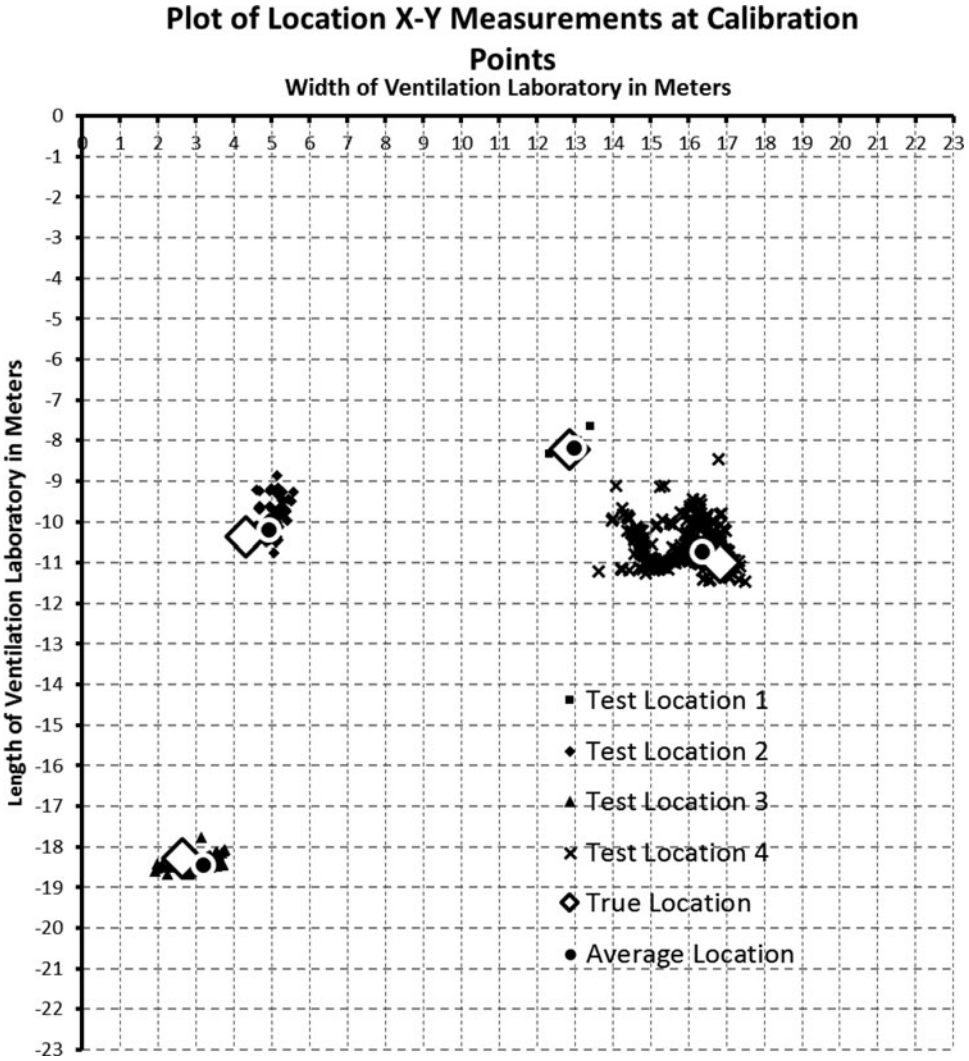


**Figure 9.** Plot of location X-Y measurements at calibration points during Run 1.

57 cm ± 31 cm through walls where the radio frequency had to penetrate drywalls (locations 2–4).

Figure 10 is a three-dimensional hazard map that was generated from the "end of shift" data. While real-time monitoring gave instantaneous location and exposure data, this hazard map displayed all the location and exposure data from the simulated work shift at a glance. The path the worker walked during the work period is immediately seen on the floor plans. The concentration can be expressed in two ways: by amplitude (or *Z* axis height) and by color with red dots being the highest concentration of 10 ppm and blue dots being the lowest concentration of 0 ppm (not colored in this graph). At a glance, one can immediately associate high concentration with location. As shown in Figure 2, there are four locations with peak heights resulting from the calibration locations at which the 10-ppm isobutylene gas was released.

The humidity and temperature sensor was not validated in this evaluation, but the manufacturer's specifications for humidity and temperature were $R^2 > 0.999$ from 20–80% and from 15–60°C. The temperature and humidity response times were 63% ≤8 sec and 30 sec,

**Table 4.** RTLS system accuracy and precision of data in terms of vector analysis.

| Calibration | True $X_1$ | True $Y_1$ | $X_2$ average | $Y_2$ average | Average Absolute Error $\sqrt{(X_1 - X_2)^2 + (Y_1 - Y_2)^2}$ | Vector Standard Deviation |
|---|---|---|---|---|---|---|
| Location 1 | 12.872 | −8.226 | 12.993 | −8.190 | 0.127 | 0.056 |
| Location 2 | 4.315 | −10.369 | 4.915 | −10.188 | 0.627 | 0.237 |
| Location 3 | 2.646 | −18.285 | 3.184 | −18.444 | 0.561 | 0.162 |
| Location 4 | 16.836 | −10.995 | 16.376 | −10.742 | 0.525 | 0.542 |

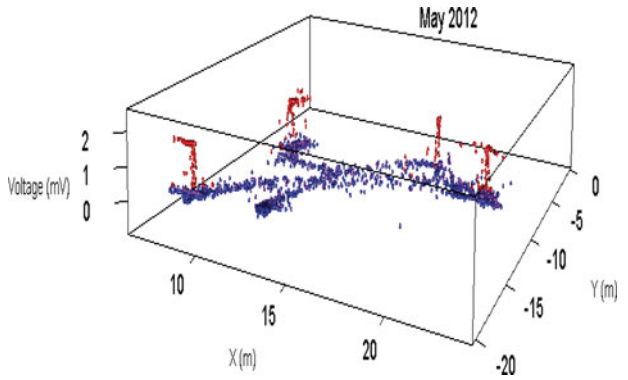


**Figure 10.** Three-dimensional graph of experimental data, using X, Y, and voltage.

respectively.[17] Therefore, within 30 sec, change was measured for all dimensions to accuracy of at least 63%. The sensitivity of the sensor for humidity and temperature was in 0.05% and 0.04°C increments, respectively, because the ADC had a 12-bit resolution. Measurements were collected at a rate of 1.4 sec/sample.

## Discussion

John Howard, Director of NIOSH, speaking on direct-reading monitors, said "While these technologies have great promise, more information is needed to understand their utility. Some of the major questions surrounding these technologies are

(1) do these monitors or applications accurately measure what they are supposed to be measuring,
(2) how are the monitors calibrated
(3) how are these technologies validated, and
(4) what are the best uses for these monitors, such as screening vs compliance."[18]

In response to these questions, the results

(1) estimated the accuracy and precision of both the chemical and location sensors,
(2) described calibration against certified isobutylene and a laser distance measuring device,
(3) documented validation method for statistical estimates of accuracy and precision, and
(4) demonstrated a DRM prototype method that combined chemical sensor and RTLS data in real time for exposure assessment.

## Conclusions

The inclusion of a real-time location system into a direct-reading method was feasible and provided enhanced exposure-assessment data. The device provided instantaneous VOC concentration with location measurements. The system provided for tracking of the device in real time with visualization of exposure concentration on a remote laptop display of the location to be monitored. Four-dimensional data plots of location and concentration provided comprehensive exposure assessment during work shifts.

## Funding

This project was funded by NIOSH. The findings and conclusions in this report are those of the author(s) and do not necessarily represent the views of the National Institute for Occupational Safety and Health.

## References

[1] **Caro, J., and M. Gallego:** Environmental and biological monitoring of volatile organic compounds in the workplace. *Chemosphere 77*(3):42–6433 (2009).
[2] **Hui, L., H. Darabi, P. Banerjee, and L. Jing:** Survey of wireless indoor positioning techniques and systems. *systems, man, and cybernetics, Part C: applications and reviews. IEEE Trans. 37*(6):1067–1080 (2007).
[3] **Lee, L.A., S.C. Soderholm, M.M. Flemmer, and J.L. Hornsby-Myers:** Field test results of an automated exposure assessment tool, the local positioning system (LPS). *J. Environ. Monit. 7*(7):736–742 (2005).
[4] **Nieto, A., and K. Dagdelen:** Improving Safety in Open Pit Mines using RTK - Differential GPS. In *Proceedings of the Seventeenth International Mining Congress And Exhibition Of Turkey*, E. Unal, and B. Unver, and E. Tercan (eds.), 2001. Ancara, Turkey, Kozan Ofset Matbaacilik San. Ve Tic. Ltd. Sti. pp. 691–696.
[5] **Boulos, M.N.K., and G. Berry:** "Real-time Locating Systems (RTLS) in Healthcare: A Condensed Primer." Available at http://www.biomedcentral.com/content/pdf/1476-072X-11-25.pdf (accessed June 30, 2015).
[6] **Huang, F-C., T-S. Shih, J-F. Lee, H-P. Chao, and P-Y Wang:** Time location analysis for exposure assessment studies of indoor workers based on active RFID technology. *J. Environ. Monitor. 12*(2):514–523 (2010).
[7] **Colwell, S.:** Business outlook — UWB location tech on a roll. *GPS World* April: 34–35 (2008).
[8] **Fleet, B., and H. Gunasingham:** Electrochemical sensors for monitoring environmental pollutants. *Talanta 39*(11):1449–1457 (1992).
[9] **Driscoll, J.N.:** Photoionization. In *Important Instrumentation and Methods for the Detection of Chemicals in the Field*, P.A. Smith, and G.W. Cook, (eds.). Falls Church, VA: American Industrial Hygiene Association, 2013. pp. 39–54.
[10] **Chen, C., K. Driggs Campbell, I. Negi, et al.:** A new sensor for the assessment of personal exposure to volatile organic compounds. *Atmosph. Environ. 54*(0):679–687 (2012).
[11] **Coffey C.C., T.A. Pearce, R.B. Lawrence, J.B. Hudnall, J.E. Slaven, and S.B. Martin:** Measurement capability of field portable organic vapor

monitoring instruments under different experimental conditions. *J. Occup. Environ. Hyg.* *6*(1):1–8 (2009).

[12] "Environment Canada - National Ambient Levels of Volatile Organic Compounds." Available at https://www.ec.gc.ca/indicateurs-indicators/default.asp?lang=en&n=95E56B3E-1 (accessed June 30, 2015).

[13] **Lee, L.A., S.C. Soderholm, M. Flemmer, J.L. Hornsby-Myers, and R. Gali:** "US Patent 7191097 B1 Method, apparatus, and system for assessing conditions." Available at http://patft.uspto.gov (accessed June 30, 2015).

[14] **Kennedy, E.R., T.J. Fischbach, R. Song, P.M. Eller, and SA. Shulman:** "Guidelines for Air Sampling and Analytical Method Development and Evaluation." Available at http://www.cdc.gov/niosh/docs/95-117/ (accessed June 30, 2015).

[15] **Bartley, D.L.:** Definition and assessment of sampling and analytical accuracy. *Ann. Occup. Hyg.* *45*(5):357–364 (2001).

[16] **NIOSH:** "Components for Evaluation of Direct-Reading Monitors for Gases and Vapors." Available at http://www.cdc.gov/niosh/docs/2012-162/pdfs/2012-162.pdf (accessed June 30, 2015).

[17] **Sensirion Co.:** "Humidity and Temperature Sensor IC Datasheet SHT1x." Available at http://www.sensirion.com/fileadmin/user_upload/customers/sensirion/Dokumente/Humidity/Sensirion_Humidity_SHT1x_Datasheet_V5.pdf (accessed June 30, 2015).

[18] **Howard, J.:** "Direct-reading and Sensor Technologies to Enable a New Era of Worker Safety, Health, Well-being, and Productivity." Available at http://www.cdc.gov/niosh/enews/enewsv12n4.html (accessed June 30, 2015).